Covert Millimeter Wave Communications Based on Beam Sweeping

Zhixiong Xing, Chenhao Qi, *Senior Member, IEEE*, Yiqun Cheng, Yiming Wu, Dongliang Lv, and Ping Li

***Abstract*— The combination of millimeter wave (mmWave) and covert communications can ensure high security for some specific circumstances. Instead of considering the covertness only in the data transmission (DT) phase for mmWave massive MIMO systems, the covertness in both the beam alignment (BA) phase and the DT phase is investigated. As a common beam training method for mmWave massive multiple-input multiple-output (MIMO), beam sweeping is adopted to obtain the optimal beam pair in the BA phase. Aiming at maximizing the average effective achievable covert rate in the DT phase, a two-stage power optimization scheme is proposed subject to the covertness and power constraints in both the BA and the DT phases. Specifically, by introducing a covertness allocation factor, closed-form expressions of the transmit power in both phases are derived according to the likelihood function of the received signal. Simulation results demonstrate that the average covert rate of MIMO is larger than that of multiple-input single-output (MISO) although the BA success rate of the former is lower than that of the latter.**

***Index Terms*— Beam sweeping, covert communications, massive multiple-input multiple-output (MIMO), millimeter wave (mmWave) communications, power optimization.**

I. Introduction

WITH the continuous evolution of artificial intelligence and big data technologies, the amount of new data generated every day around the world is growing exponentially while wireless communication networks are playing an increasingly important role. Meanwhile, the security of wireless communication networks such as Internet of Things (IoT) and Internet of Vehicles (IoV) is receiving extensive attention from academia and industry [1]. Due to the large bandwidth and high directivity of millimeter wave (mmWave) communications and the marvelous spectral efficiency of massive multiple-input multiple-output (MIMO), mmWave massive MIMO is considered as one of the key technologies for the next-generation mobile communications [2], [3]. On the other hand, covert communications can hide the existence of wireless communications, which can effectively improve the security [4]. The above two aspects motivate the study of covert mmWave wireless communications.

The covert mmWave communication system is first studied from the perspective of communication principle, where the advantages of covert mmWave communications compared to the conventional low-frequency counterparts are demonstrated [5]. In [6], a legitimate user working in full-duplex mode and a warden operating in half-duplex mode are considered, where the covert rate for both single and multiple data streams are maximized by jointly optimizing the hybrid beamforming, transmit power and analog jamming. In [7], a multicast mmWave multiple-input single-output (MISO) system with multiple legitimate users is investigated, where the minimum covert rate is maximized subject to the power and covertness constraint. In [8], an unmanned aerial vehicle (UAV)-aided covert mmWave communication system is considered, where the number of beams, transmit power and flight altitude of the UAV are jointly optimized to maximize the average throughput subject to a covertness constraint. Nevertheless, the above studies consider the covertness only in the data transmission (DT) phase of the mmWave massive MIMO while the beam alignment (BA) phase also has a risk of exposing the communication process. In [9], the beam training duration, training power and data transmission power are jointly optimized to maximize the effective covert rate under the covertness constraint, where the average effective achievable covert rate in the case of beam misalignment is omitted and the generalized flat-top beam and single-path line of sight (LOS) channel are considered.

In this letter, we further investigate the covertness in both the BA and the DT phases for mmWave massive MIMO system. The main contributions of this letter are summarized as follows. 1) Based on [9], we further consider the discrete Fourier transform (DFT) codebook, the multipath mmWave MIMO channel, and the average effective achievable covert rate in the case of beam misalignment. 2) The transmit power is optimized separately for the BA and the DT phases and the closed-form expressions of the transmit power in both phases are derived.

Notations: Symbols for vectors (lower case) and matrices (upper case) are in boldface. For a vector $\boldsymbol{a}$, $[\boldsymbol{a}]_m$, $\boldsymbol{a}^{\mathrm{H}}$ and $\|\boldsymbol{a}\|_2$ denote its mth entry, conjugate transpose and l_2-norm, respectively. $\mathcal{D}(\mathcal{A}||\mathcal{B})$ denotes the relative entropy of $\mathcal{A}$ to $\mathcal{B}$. $\boldsymbol{I}_K$ denotes an $K \times K$ identity matrix. $\mathcal{CN}(p, \sigma^2)$ denotes the complex Gaussian distribution with the mean being p and the variance being σ^2. Symbol $\mathbb{C}$ denotes the set of complex-valued numbers. $|x|$ denotes the modulus of complex number x. $a \bmod b$ denotes the remainder of a to b.

II. System Model and Problem Formulation

We consider a downlink narrowband single-user covert mmWave communication system, including a base station

Manuscript received 16 February 2023; accepted 13 March 2023. Date of publication 15 March 2023; date of current version 10 May 2023. This work is supported in part by National Natural Science Foundation of China under Grants 62071116 and U22B2007, and by National Key Research and Development Program of China under Grant 2021YFB2900404. The associate editor coordinating the review of this letter and approving it for publication was G. Interdonato. *(Corresponding author: Chenhao Qi.)*

Zhixiong Xing is with the National Mobile Communications Research Laboratory, School of Information Science and Engineering and the School of Cyber Science and Engineering, Southeast University, Nanjing 210096, China (e-mail: zxxing@seu.edu.cn).

Chenhao Qi and Yiqun Cheng are with the National Mobile Communications Research Laboratory, School of Information Science and Engineering, Southeast University, Nanjing 210096, China (e-mail: qch@seu.edu.cn; 220194710@seu.edu.cn).

Yiming Wu, Dongliang Lv, and Ping Li are with ZTE Corporation, Shenzhen 518057, China (e-mail: wu.yiming1@zte.com.cn; lv.dongliang@zte.com.cn; li.ping6@zte.com.cn).

Digital Object Identifier 10.1109/LCOMM.2023.3257568

1558-2558 © 2023 IEEE. Personal use is permitted, but republication/redistribution requires IEEE permission.
See https://www.ieee.org/publications/rights/index.html for more information.

Authorized licensed use limited to: Southeast University. Downloaded on May 10,2023 at 08:07:31 UTC from IEEE Xplore. Restrictions apply.

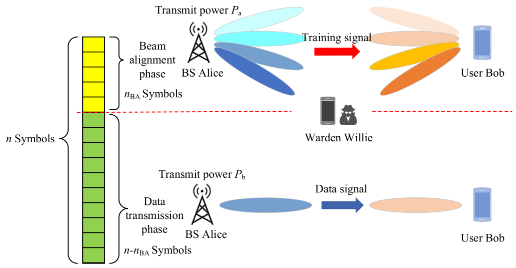

Fig. 1. System model of covert mmWave wireless communications based on beam sweeping.

Alice, a legitimate user Bob and a warden Willie. Alice and Bob are equipped with N_t and N_r antennas which are placed in uniform linear arrays (ULAs) with half wavelength intervals. Note that Willie is always greedy and nimble and is assumed to be equipped with a single antenna to monitor omni-directional signal [9]. As shown in Fig. 1, we consider a complete mmWave wireless communication process, including the BA and the DT phases. Note that the coincidence of Willie's and Bob's azimuths relative to Alice is not considered, which is to ensure that the azimuth difference between Willie and Bob relative to Alice is greater than the minimum mainlobe coverage of Alice's transmit beam.

According to the widely used Saleh-Valenzuela (SV) narrowband channel model [10], the channel $\boldsymbol{H}_\mathrm{ab} \in \mathbb{C}^{N_\mathrm{r}\times N_\mathrm{t}}$ between Alice and Bob can be expressed as

$$\boldsymbol{H}_\mathrm{ab} = \sqrt{\frac{N_\mathrm{t}N_\mathrm{r}}{L^{(\mathrm{ab})}}}\sum_{l=1}^{L^{(\mathrm{ab})}} \alpha_l^{(\mathrm{ab})}\boldsymbol{a}(N_\mathrm{r},\varphi_l^{(\mathrm{ab})})\boldsymbol{a}^\mathrm{H}(N_\mathrm{t},\phi_l^{(\mathrm{ab})}), \quad (1)$$

where $L^{(\mathrm{ab})}$ denotes the number of multipath components (MPCs) between Alice and Bob. $\alpha_l^{(\mathrm{ab})}$, $\varphi_l^{(\mathrm{ab})}$ and $\phi_l^{(\mathrm{ab})}$ denote the complex gain, angle of arrival (AoA) and angle of departure (AoD) of the lth MPC, respectively. $\boldsymbol{a}(N,\phi)$ is the channel steering vector defined as

$$\boldsymbol{a}(N,\phi) \triangleq \frac{1}{\sqrt{N}}[1, e^{j\pi\phi},\ldots,e^{j(N-1)\pi\phi}]^\mathrm{T}, \phi\in[-1,1]. \quad (2)$$

We assume that Alice and Bob can communicate at most n symbols during a time frame in which the channel remains quasi-static. Meanwhile, beam sweeping is adopted to accomplish BA. Note that the beam sweeping aims at finding the beam pair best fit for $\boldsymbol{H}_\mathrm{ab}$, instead of directly estimating $\boldsymbol{H}_\mathrm{ab}$. During the BA phase, the received signal of Bob in the mth beam training can be expressed as

$$[\boldsymbol{y}_\mathrm{ab}^\mathrm{BA}]_m = \sqrt{P_\mathrm{a}}\boldsymbol{f}_m^\mathrm{H}\boldsymbol{H}_\mathrm{ab}\boldsymbol{w}_m[\boldsymbol{x}_\mathrm{p}]_m + z_\mathrm{b}, m\in[1:M], \quad (3)$$

where $\boldsymbol{y}_\mathrm{ab}^\mathrm{BA} \in \mathbb{C}^{M\times 1}$ denotes Bob's received signal vector, P_a denotes the transmit power of Alice, $\boldsymbol{x}_\mathrm{p} \in \mathbb{C}^{M\times 1}$ with $\left|[\boldsymbol{x}_\mathrm{p}]_m\right| = 1$ denotes the beam training symbol vector, and $z_\mathrm{b} \sim \mathcal{CN}(0,\sigma_\mathrm{b}^2)$ denotes the additive white Gaussian noise (AWGN) at Bob in the BA phase. $\boldsymbol{w}_m \in \mathbb{C}^{N_\mathrm{t}\times 1}$ and $\boldsymbol{f}_m \in \mathbb{C}^{N_\mathrm{r}\times 1}$ denote the codewords which are selected by Alice and Bob from their codebooks, respectively, and then used for the mth beam training. $M \triangleq M_\mathrm{a}M_\mathrm{b}$ is the number of all beam pairs tested by beam sweeping, where M_a and M_b denote the size of Alice's and Bob's DFT codebook, respectively. Note that the DFT codebook is more popularly used than the generalized flat-top beam [9] in mmWave MIMO communications, since the former achieves better covertness than the latter with larger beam gain and narrower beamwidth.

The DFT codebook $\boldsymbol{U}$ of size M_a can be expressed as [10]

$$\boldsymbol{U} \triangleq [\boldsymbol{a}(M_\mathrm{a},\theta_0), \boldsymbol{a}(M_\mathrm{a},\theta_1),\ldots,\boldsymbol{a}(M_\mathrm{a},\theta_{M_\mathrm{a}-1})], \quad (4)$$

where $\theta_i = -1+(2i+1)/M_\mathrm{a}, i = 0,\ldots,M_\mathrm{a}-1$. Each column in $\boldsymbol{U}$ is a codeword with beamwidth being $2/M_\mathrm{a}$ and the M_a codewords uniformly cover the angular space of $[-1,1]$.

We define the resulted optimal beam pair index obtained by beam sweeping as

$$\hat{m} = \arg\max_{m\in[1:M]} \left|[\boldsymbol{y}_\mathrm{ab}^\mathrm{BA}]_m\right|. \quad (5)$$

Therefore, the received signal of Bob in the DT phase can be expressed as

$$y_\mathrm{ab}^\mathrm{DT} = \sqrt{P_\mathrm{b}}\boldsymbol{f}_{\hat{m}}^\mathrm{H}\boldsymbol{H}_\mathrm{ab}\boldsymbol{w}_{\hat{m}}x_\mathrm{d} + z_\mathrm{b}, \quad (6)$$

where P_b is the transmit power of Alice in the DT phase and $x_\mathrm{d} \sim \mathcal{CN}(0,1)$ is the effective data symbol.

Then the average effective achievable covert rate can be expressed as

$$R = \left(\frac{n-n_\mathrm{BA}}{n}\right)\log_2\left(1+\frac{P_\mathrm{b}\left|\boldsymbol{f}_{\hat{m}}^\mathrm{H}\boldsymbol{H}_\mathrm{ab}\boldsymbol{w}_{\hat{m}}\right|^2}{\sigma_\mathrm{b}^2}\right), \quad (7)$$

where $n_\mathrm{BA} = M = N_\mathrm{t}N_\mathrm{r}$ is the number of symbols used in the BA phase. Note that (7) includes the average effective achievable covert rate even in the case of beam misalignment, e.g., in the case that the noise power is much larger than the signal power.

Similarly, the received signal of Willie in the BA and the DT phases can be expressed as

$$[\boldsymbol{y}_\mathrm{aw}^\mathrm{BA}]_m = \sqrt{P_\mathrm{a}}\boldsymbol{h}_\mathrm{aw}\boldsymbol{w}_m[\boldsymbol{x}_\mathrm{p}]_m + z_\mathrm{w}, m\in[1:M], \quad (8)$$

$$y_\mathrm{aw}^\mathrm{DT} = \sqrt{P_\mathrm{b}}\boldsymbol{h}_\mathrm{aw}\boldsymbol{w}_{\hat{m}}x_\mathrm{d} + z_\mathrm{w}, \quad (9)$$

where $z_\mathrm{w} \sim \mathcal{CN}(0,\sigma_\mathrm{w}^2)$ denotes the AWGN at Willie. $\boldsymbol{h}_\mathrm{aw} \in \mathbb{C}^{1\times N_\mathrm{t}}$ denoting the channel between Alice and Willie, can be expressed as

$$\boldsymbol{h}_\mathrm{aw} = \sqrt{\frac{N_\mathrm{t}}{L^{(\mathrm{aw})}}}\sum_{l=1}^{L^{(\mathrm{aw})}} \alpha_l^{(\mathrm{aw})}\boldsymbol{a}^\mathrm{H}(N_\mathrm{t},\phi_l^{(\mathrm{aw})}), \quad (10)$$

where $L^{(\mathrm{aw})}$ denotes the number of MPCs between Alice and Willie. $\alpha_l^{(\mathrm{aw})}$ and $\phi_l^{(\mathrm{aw})}$ denote the complex gain and the AoD of the lth MPC, respectively.

Willie's detection of Alice's signal transmission can be classified as a binary hypothesis testing problem. It can be expressed as

$$\begin{cases}\mathcal{H}_0 : \boldsymbol{y}_\mathrm{aw} = \boldsymbol{z}_\mathrm{w},\\ \mathcal{H}_1 : \boldsymbol{y}_\mathrm{aw} = \boldsymbol{s} + \boldsymbol{z}_\mathrm{w},\end{cases} \quad (11)$$

where $\boldsymbol{y}_\mathrm{aw} \in \mathbb{C}^{n\times 1}$ denotes the received signal vector of Willie, $\boldsymbol{s} \in \mathbb{C}^{n\times 1}$ denotes the leaked signal vector of Alice during the BA and the DT phases and $\boldsymbol{z}_\mathrm{w} \in \mathbb{C}^{n\times 1}$ is the channel noise vector. $\mathcal{H}_0$ denotes the null hypothesis and $\mathcal{H}_1$ denotes the alternative hypothesis [9].

Authorized licensed use limited to: Southeast University. Downloaded on May 10,2023 at 08:07:31 UTC from IEEE Xplore. Restrictions apply.

Willie needs to perform the binary judement $\mathcal{D}_0$ and $\mathcal{D}_1$. We assume that $\mathcal{H}_0$ and $\mathcal{H}_1$ have the same prior probability [4]. Then the overall detection error probability is

$$\xi = \frac{\alpha + \beta}{2}, \tag{12}$$

where $\alpha \triangleq \Pr(\mathcal{D}_1 = \mathcal{H}_1|\mathcal{H}_0)$ denotes the false alarm probability and $\beta \triangleq \Pr(\mathcal{D}_0 = \mathcal{H}_0|\mathcal{H}_1)$ denotes the missed detection probability.

Assuming that the minimum overall detection error probability is ξ^*, we can express the covertness constraint as

$$\xi^* \geq 1 - \epsilon, \tag{13}$$

where $\epsilon > 0$ represents the requirement of the covertness.

According to the Pinsker's inequality [9], the above covertness constraint can be converted into

$$\mathcal{D}(\mathcal{P}_0||\mathcal{P}_1) \leq 2\epsilon^2, \tag{14}$$

where $\mathcal{P}_0$ and $\mathcal{P}_1$ denote the likelihood function (LF) of Willie's received signal under $\mathcal{H}_0$ and $\mathcal{H}_1$, respectively.

By introducing a covertness allocation factor $K \in [0, 1]$, the optimization problem of the BA phase is expressed as

$$\max_{P_\mathrm{a}} \ R, \tag{15a}$$
$$\text{s.t.} \ \ \mathcal{D}(\mathcal{P}_0^\mathrm{BA}||\mathcal{P}_1^\mathrm{BA}) \leq 2K\epsilon^2, \tag{15b}$$
$$P_\mathrm{a} \leq P_\mathrm{max}^\mathrm{BA}, \tag{15c}$$

where $P_\mathrm{max}^\mathrm{BA}$ is the maximum transmit power in the BA phase, $\mathcal{P}_0^\mathrm{BA}$ and $\mathcal{P}_1^\mathrm{BA}$ denote the LF of n_BA received symbols by Willie under $\mathcal{H}_0$ and $\mathcal{H}_1$, respectively.

Note that the expression of the average effective achievable covert rate R in (7) doesn't have parameter P_a, but P_a has an influence on R obviously. In particular, larger P_a can improve the BA success rate [10], which further enhances the beamforming gain and increases the average effective achievable covert rate. Accordingly, (15) can be rewritten as

$$\max_{P_\mathrm{a}} \ P_\mathrm{a}, \tag{16a}$$
$$\text{s.t.} \ \ \mathcal{D}(\mathcal{P}_0^\mathrm{BA}||\mathcal{P}_1^\mathrm{BA}) \leq 2K\epsilon^2, \tag{16b}$$
$$P_\mathrm{a} \leq P_\mathrm{max}^\mathrm{BA}. \tag{16c}$$

Similarly, the optimization problem of the DT phase can be expressed as

$$\max_{P_\mathrm{b}} \ R, \tag{17a}$$
$$\text{s.t.} \ \ \mathcal{D}(\mathcal{P}_0||\mathcal{P}_1) \leq 2\epsilon^2, \tag{17b}$$
$$P_\mathrm{b} \leq P_\mathrm{max}^\mathrm{DT}, \tag{17c}$$

where $P_\mathrm{max}^\mathrm{DT}$ is the maximum transmit power in the DT phase and (17b) indicates that the covertness constraint of both the BA and the DT phases should be taken into consideration in the DT phase.

III. TWO-STAGE POWER OPTIMIZATION SCHEME

In this section, we propose a two-stage power optimization scheme for (16) and (17) and give a closed-form solution to P_a and P_b.

During the BA phase, the elements of $\boldsymbol{y}_\mathrm{aw}^\mathrm{BA}$ are i.i.d. $\sim \mathcal{CN}(0, \sigma_\mathrm{w}^2)$ under $\mathcal{H}_0$, where Willie only receives the noise signal. Hence, we have

$$\mathcal{P}_0^\mathrm{BA} = \prod_{i=1}^{n_\mathrm{BA}} \frac{1}{\pi\sigma_\mathrm{w}^2} e^{-\frac{\left|[\boldsymbol{y}_\mathrm{aw}^\mathrm{BA}]_i\right|^2}{\sigma_\mathrm{w}^2}}. \tag{18}$$

Note that the noise variance of $\boldsymbol{h}_\mathrm{aw}$ is assumed to be known, i.e., the noise uncertainty is not considered in this letter and the system's uncertainty to Willie can be ensured by the finite number of transmit symbols. It has already been proved that the optimal number of transmit symbols is the maximum number of symbols which can be transmitted during a time frame [11].

Similarly, Willie can receive both Alice's beam training symbols and the noise signal under $\mathcal{H}_1$. Hence, the elements of $\boldsymbol{y}_\mathrm{aw}^\mathrm{BA}$ are i.i.d. $\sim \mathcal{CN}(p_i, \sigma_\mathrm{w}^2)$ under $\mathcal{H}_1$. Consequently, we have

$$\mathcal{P}_1^\mathrm{BA} = \prod_{i=1}^{n_\mathrm{BA}} \frac{1}{\pi\sigma_\mathrm{w}^2} e^{-\frac{\left|[\boldsymbol{y}_\mathrm{aw}^\mathrm{BA}]_i - p_i\right|^2}{\sigma_\mathrm{w}^2}}, \tag{19}$$

where $p_i = \sqrt{P_\mathrm{a}}\boldsymbol{h}_\mathrm{aw}\boldsymbol{w}_i$, and $\boldsymbol{w}_i$ is the codeword from Alice's codebook and used to transmit the ith training symbol.

According to [9], both $\left|[\boldsymbol{y}_\mathrm{aw}^\mathrm{BA}]_i\right|^2$ and $\left|[\boldsymbol{y}_\mathrm{aw}^\mathrm{BA}]_i - p_i\right|^2$ obey noncentral chi-squared distribution with degrees of freedom (DoFs) $k = 2$. As a result, (16b) can be converted into

$$\mathcal{D}(\mathcal{P}_0^\mathrm{BA}||\mathcal{P}_1^\mathrm{BA}) = \mathbb{E}_{\mathcal{P}_0^\mathrm{BA}}\left\{\ln\mathcal{P}_0^\mathrm{BA} - \ln\mathcal{P}_1^\mathrm{BA}\right\} \tag{20a}$$
$$= \frac{\sum_{i=1}^{n_\mathrm{BA}} p_i^2}{\sigma_\mathrm{w}^2} \leq 2K\epsilon^2, \tag{20b}$$

where $\mathbb{E}_\mathcal{P}\{r\}$ denotes the mathematical expectation of r under the LF $\mathcal{P}$.

By substituting (20b) into (16),we can rewrite (16) as

$$\max_{P_\mathrm{a}} \ P_\mathrm{a}, \tag{21a}$$
$$\text{s.t.} \ \ \frac{\sum_{i=1}^{n_\mathrm{BA}} p_i^2}{\sigma_\mathrm{w}^2} \leq 2K\epsilon^2, \tag{21b}$$
$$P_\mathrm{a} \leq P_\mathrm{max}^\mathrm{BA}. \tag{21c}$$

Note that the left hand side (LHS) of (21b) can be further derived as

$$\frac{\sum_{i=1}^{n_\mathrm{BA}} p_i^2}{\sigma_\mathrm{w}^2} = \frac{\sum_{i=1}^{N_\mathrm{t}N_\mathrm{r}} P_\mathrm{a}\left|\boldsymbol{h}_\mathrm{aw}\boldsymbol{w}_{f(i)}\right|^2}{\sigma_\mathrm{w}^2} \overset{(a)}{=} \frac{N_\mathrm{r}P_\mathrm{a}\|\boldsymbol{h}_\mathrm{aw}\|_2^2}{\sigma_\mathrm{w}^2}, \tag{22}$$

where

$$f(i) \triangleq \begin{cases} N_\mathrm{t}, & \text{if } i \bmod N_\mathrm{t} = 0, \\ i \bmod N_\mathrm{t}, & \text{else.} \end{cases} \tag{23}$$

In particular, (a) can be derived by

$$\sum_{i=1}^{N_\mathrm{t}N_\mathrm{r}} \left|\boldsymbol{h}_\mathrm{aw}\boldsymbol{w}_{f(i)}\right|^2 = \|\boldsymbol{h}_\mathrm{aw}\boldsymbol{W}\|_2^2 = \boldsymbol{h}_\mathrm{aw}\boldsymbol{W}\boldsymbol{W}^\mathrm{H}\boldsymbol{h}_\mathrm{aw}^\mathrm{H}$$
$$= N_\mathrm{r}\boldsymbol{h}_\mathrm{aw}\boldsymbol{h}_\mathrm{aw}^\mathrm{H} = N_\mathrm{r}\|\boldsymbol{h}_\mathrm{aw}\|_2^2, \tag{24}$$

Authorized licensed use limited to: Southeast University. Downloaded on May 10,2023 at 08:07:31 UTC from IEEE Xplore. Restrictions apply.

where $\boldsymbol{W} \triangleq [\boldsymbol{W}_1, \boldsymbol{W}_2, \ldots, \boldsymbol{W}_{N_\mathrm{r}}]$ and $\boldsymbol{W}_1 = \boldsymbol{W}_2 = \ldots = \boldsymbol{W}_{N_\mathrm{r}} = [\boldsymbol{w}_1, \boldsymbol{w}_2, \ldots, \boldsymbol{w}_{N_\mathrm{t}}]$. Obviously, we have $\boldsymbol{W}_j \boldsymbol{W}_j^\mathrm{H} = \boldsymbol{I}_{N_\mathrm{t}}$ for $j = 1, 2, \ldots, N_\mathrm{r}$ and consequently $\boldsymbol{W}\boldsymbol{W}^\mathrm{H} = N_\mathrm{r}\boldsymbol{I}_{N_\mathrm{t}}$.

Hence, the solution of P_a for (21) can be obtained by

$$P_\mathrm{a} = \min\left(P_{\max}^{\mathrm{BA}}, \frac{2K\epsilon^2\sigma_\mathrm{w}^2}{N_\mathrm{r}\|\boldsymbol{h}_\mathrm{aw}\|_2^2}\right). \tag{25}$$

Note that we only need $\|\boldsymbol{h}_\mathrm{aw}\|_2$ instead of knowing $\boldsymbol{h}_\mathrm{aw}$, where $\|\boldsymbol{h}_\mathrm{aw}\|_2$ can be determined according to [6].

For the optimization of P_b in (17), we need to consider the observations over the entire time frame, i.e., n symbols. The LF of Willie's received signal under $\mathcal{H}_0$ can be expressed as

$$\mathcal{P}_0 = \mathcal{P}_0^{\mathrm{BA}} \times \mathcal{P}_0^{\mathrm{DT}} = \prod_{i=1}^{n} \frac{1}{\pi\sigma_\mathrm{w}^2} e^{-\frac{\left|[\boldsymbol{y}_\mathrm{aw}]_i\right|^2}{\sigma_\mathrm{w}^2}}, \tag{26}$$

where $\mathcal{P}_0^{\mathrm{DT}}$ is the LF of the received signal in the DT phase under $\mathcal{H}_0$ and $\boldsymbol{y}_\mathrm{aw} \in \mathbb{C}^{n\times 1}$ is the received signal vector over the entire time frame.

Because the effective data symbol $x_\mathrm{d} \sim \mathcal{CN}(0,1)$, the elements of $\boldsymbol{y}_\mathrm{aw}^{\mathrm{DT}} \in \mathbb{C}^{(n-n_{\mathrm{BA}})\times 1}$ under $\mathcal{H}_1$ are i.i.d. $\sim \mathcal{CN}(0, \sigma_\mathrm{w}^2 + P_\mathrm{b}\left|\boldsymbol{h}_\mathrm{aw}\boldsymbol{w}_{\hat{m}}\right|^2)$. Then the LF of $\boldsymbol{y}_\mathrm{aw}^{\mathrm{DT}}$ can be expressed as

$$\mathcal{P}_1^{\mathrm{DT}} = \prod_{i=n_{\mathrm{BA}}+1}^{n} \frac{1}{\pi(\sigma_\mathrm{w}^2 + P_\mathrm{b}\left|\boldsymbol{h}_\mathrm{aw}\boldsymbol{w}_{\hat{m}}\right|^2)} e^{-g(i)}, \tag{27}$$

where

$$g(i) \triangleq \frac{\left|[\boldsymbol{y}_\mathrm{aw}^{\mathrm{DT}}]_i\right|^2}{\sigma_\mathrm{w}^2 + P_\mathrm{b}\left|\boldsymbol{h}_\mathrm{aw}\boldsymbol{w}_{\hat{m}}\right|^2}. \tag{28}$$

In this way, the LF of Willie's received signal under $\mathcal{H}_1$ over the entire time frame can be expressed as

$$\mathcal{P}_1 = \mathcal{P}_1^{\mathrm{BA}} \times \mathcal{P}_1^{\mathrm{DT}}. \tag{29}$$

Accordingly, the relative entropy of $\mathcal{P}_0$ to $\mathcal{P}_1$ is

$$\begin{aligned}\mathcal{D}(\mathcal{P}_0||\mathcal{P}_1) = {} & (n - n_{\mathrm{BA}})\ln\left(1 + \frac{P_\mathrm{b}\left|\boldsymbol{h}_\mathrm{aw}\boldsymbol{w}_{\hat{m}}\right|^2}{\sigma_\mathrm{w}^2}\right) \\ & + \mathcal{D}(\mathcal{P}_0^{\mathrm{BA}}||\mathcal{P}_1^{\mathrm{BA}}) - (n - n_{\mathrm{BA}})\frac{2}{\sigma_\mathrm{w}^2} \\ & + (n - n_{\mathrm{BA}})\frac{2}{\sigma_\mathrm{w}^2}\frac{\sigma_\mathrm{w}^2}{\sigma_\mathrm{w}^2 + P_\mathrm{b}\left|\boldsymbol{h}_\mathrm{aw}\boldsymbol{w}_{\hat{m}}\right|^2}. \end{aligned} \tag{30}$$

By substituting (30) into (17b) and then introducing

$$\delta \triangleq \frac{2\epsilon^2 - \mathcal{D}(\mathcal{P}_0^{\mathrm{BA}}||\mathcal{P}_1^{\mathrm{BA}})}{n - n_{\mathrm{BA}}}, \tag{31}$$

$$x \triangleq 1 + \frac{P_\mathrm{b}\left|\boldsymbol{h}_\mathrm{aw}\boldsymbol{w}_{\hat{m}}\right|^2}{\sigma_\mathrm{w}^2} \geq 1, \tag{32}$$

we can convert (17b) into

$$\ln(x) + \frac{2}{\sigma_\mathrm{w}^2}\frac{1}{x} \leq \frac{2}{\sigma_\mathrm{w}^2} + \delta. \tag{33}$$

Using a second-order Taylor expansion at $x = 1$ on the LHS of (33), we can convert (33) into

$$\left(\frac{2}{\sigma_\mathrm{w}^2} - \frac{1}{2}\right)x^2 + \left(2 - \frac{6}{\sigma_\mathrm{w}^2}\right)x + \frac{6}{\sigma_\mathrm{w}^2} - \frac{3}{2} \leq \frac{2}{\sigma_\mathrm{w}^2} + \delta. \tag{34}$$

Algorithm 1 Two-Stage Power Optimization

Input: $N_\mathrm{t}, N_\mathrm{r}, n, \epsilon, K, Q, P_{\max}^{\mathrm{BA}}, P_{\max}^{\mathrm{DT}}$.
Generate the DFT codebooks for signal transmitting and receiving. Set $n_{\mathrm{BA}} = N_\mathrm{t}N_\mathrm{r}$.
Initialize the channel SNR κ_{ab} and κ_{aw}.
Calculate σ_b^2 and σ_w^2.
Obtain P_a based on (25).
Obtain P_b based on (39).
Output: P_a, P_b.

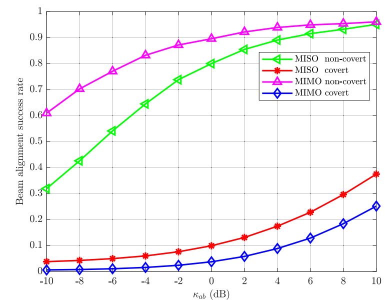

Fig. 2. BA success rate of different scenarios.

By solving the unary quadratic inequality of (34), we have

$$x \leq \frac{3t - 2 + \sqrt{\Delta}}{2t - 1}, \tag{35}$$

where $t = 2/\sigma_\mathrm{w}^2$ and $\Delta = t^2 + (4\delta - 2)t + 1 - 2\delta$.

Based on (32), we have

$$P_\mathrm{b} \leq \frac{\frac{3t-2+\sqrt{\Delta}}{2t-1}\sigma_\mathrm{w}^2 - \sigma_\mathrm{w}^2}{\left|\boldsymbol{h}_\mathrm{aw}\boldsymbol{w}_{\hat{m}}\right|^2}. \tag{36}$$

According to the Cauchy-Schwarz inequality [12], the denominator of the right hand side (RHS) of (36) can be scaled to

$$\left|\boldsymbol{h}_\mathrm{aw}\boldsymbol{w}_{\hat{m}}\right|^2 \leq \boldsymbol{h}_\mathrm{aw}\boldsymbol{h}_\mathrm{aw}^\mathrm{H}\boldsymbol{w}_{\hat{m}}\boldsymbol{w}_{\hat{m}}^\mathrm{H} = \boldsymbol{h}_\mathrm{aw}\boldsymbol{h}_\mathrm{aw}^\mathrm{H} = \|\boldsymbol{h}_\mathrm{aw}\|_2^2. \tag{37}$$

Subsequently, (36) can be converted into

$$P_\mathrm{b} \leq \frac{\frac{3t-2+\sqrt{\Delta}}{2t-1}\sigma_\mathrm{w}^2 - \sigma_\mathrm{w}^2}{\|\boldsymbol{h}_\mathrm{aw}\|_2^2}. \tag{38}$$

By introducing a scaling factor $Q \in (0, 1]$, the solution of P_b for (17) can be obtained by

$$P_\mathrm{b} = \min\left(P_{\max}^{\mathrm{DT}}, \frac{\frac{3t-2+\sqrt{\Delta}}{2t-1}\sigma_\mathrm{w}^2 - \sigma_\mathrm{w}^2}{Q\|\boldsymbol{h}_\mathrm{aw}\|_2^2}\right). \tag{39}$$

Note that the choice of Q is related to N_t. Larger N_t causes bigger mainlobe gain and smaller sidelobe gain of the DFT codeword, which further decreases the value of $\left|\boldsymbol{h}_\mathrm{aw}\boldsymbol{w}_{\hat{m}}\right|^2/\|\boldsymbol{h}_\mathrm{aw}\|_2^2$. Therefore, a small Q is preferred.

The detailed steps of the two-stage power optimization scheme are summarized in **Algorithm 1**.

IV. Simulation Results

To evaluate the system performance, the channel between Alice and Bob (or Willie) is supposed to have three MPCs, i.e., $L^{(\mathrm{ab})} = L^{(\mathrm{aw})} = 3$, including a LOS path and two non-LOS (NLOS) paths. The channel gains of LOS paths obey $\alpha_1^{(\mathrm{ab})}, \alpha_1^{(\mathrm{aw})} \sim \mathcal{CN}(0, 1)$ and that of NLOS paths

Authorized licensed use limited to: Southeast University. Downloaded on May 10,2023 at 08:07:31 UTC from IEEE Xplore. Restrictions apply.

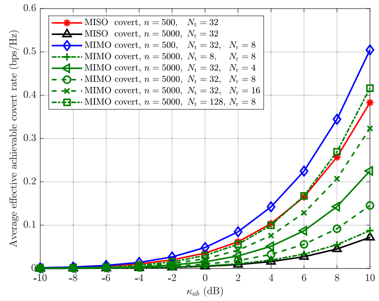

Fig. 3. Average effective achievable covert rate under different $\kappa_{\rm ab}$.

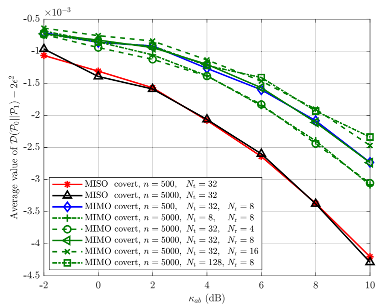

Fig. 4. Average value of $\mathcal{D}(\mathcal{P}_0||\mathcal{P}_1) - 2\epsilon^2$ under different $\kappa_{\rm ab}$.

obey $\alpha_2^{(\rm ab)}, \alpha_3^{(\rm ab)}, \alpha_2^{(\rm aw)}, \alpha_3^{(\rm aw)} \sim \mathcal{CN}(0, 0.01)$. The AoDs and AoAs of all MPCs obey uniform distribution in $[-1, 1]$. Besides, the channel signal-to-noise ratio (SNR) is defined as $\kappa \triangleq \mathbb{E}\{|\alpha|^2\}/\sigma^2$, where α denotes the complex channel gain of LOS path and σ^2 denotes the noise variance. $|\alpha|^2$ obeys a chi-squared distribution with DoFs $k = 2$ since $\alpha \sim \mathcal{CN}(0, 1)$. Hence, we have $\mathbb{E}\{|\alpha|^2\} = 2$ and $\kappa = 2/\sigma^2$. The maximum transmit power in the BA and the DT phases is set to be $P_{\max}^{\rm BA} = P_{\max}^{\rm DT} = 1$. The value of Q is set as 0.13, 0.033 and 0.0083 for $N_{\rm t} = 8$, $N_{\rm t} = 32$ and $N_{\rm t} = 128$, respectively. K is set as 0.375 and 0.475 for MISO and MIMO, respectively. And ϵ is set as 0.1.

As shown in Fig. 2, we evaluate the BA success rate under different $\kappa_{\rm ab}$ for four different scenarios. We fix $n = 500$, $N_{\rm t} = 32$ and $N_{\rm r} = 8$. It can be seen that the BA success rate of covert scenario is much lower than that of non-covert scenario because the transmit power of the BA phase under covert scenario is smaller than that of non-covert scenario in order to satisfy the covertness constraint. In addition, MIMO covert scenario needs to send $N_{\rm r}$ times training symbols of MISO covert scenario while the former still needs to satisfy the same covertness constraint as the latter. Hence, MIMO covert scenario needs to reduce $P_{\rm a}$, which further decreases the BA success rate. In this way, the BA success rate of MISO is higher than that of MIMO under covert scenario.

As shown in Fig. 3, we further evaluate the average effective achievable covert rate under different $\kappa_{\rm ab}$ for MISO and MIMO. Different numbers of transmitting and receiving antennas and symbols are considered. It is shown that the average covert rate increases with $\kappa_{\rm ab}$ for both MISO and MIMO. Besides, the average covert rate of MIMO is higher than that of MISO with the same number of symbols. The gap between MIMO and MISO enlarges with the increase of $\kappa_{\rm ab}$, since the beamforming gain of MIMO is much larger than that of MISO. When n raises from 500 to 5000, the average covert rate decreases, since the number of transmit symbols increases and $P_{\rm b}$ decreases to satisfy the same covertness constraint in the DT phase. Moreover, the average covert rate gets larger with more transmitting and receiving antennas. More antennas contribute to narrower beams, larger mainlobe gain and smaller sidelobe gain, which further reduces the chance of being detected by Willie and improves the average covert rate.

As shown in Fig. 4, we compare the average value of the covertness constraint under different $\kappa_{\rm ab}$ under the same settings as Fig. 3. It is seen that the covertness constraint can be well satisfied. The value of $\mathcal{D}(\mathcal{P}_0||\mathcal{P}_1) - 2\epsilon^2$ decreases as $\kappa_{\rm ab}$ increases, since larger $\kappa_{\rm ab}$ results in higher BA success rate, which further decreases the chance of being detected by Willie. In particular, the value of $\mathcal{D}(\mathcal{P}_0||\mathcal{P}_1) - 2\epsilon^2$ for MIMO is larger than that for MISO and gets larger with more transmitting and receiving antennas, which demonstrates that MIMO achieves a better tradeoff between the covertness and the data rate than MISO.

V. Conclusion

In this letter, we have considered the covertness in both the BA and the DT phases for mmWave MIMO communications, where the BA phase adopts the beam sweeping method. Then we have proposed a two-stage power optimization scheme and given the closed-form solutions of the transmit power for aforementioned two phases. In the future, we will extend our work to mmWave MIMO with hybrid beamforming.

References

[1] Z. Liu, J. Liu, Y. Zeng, and J. Ma, "Covert wireless communication in IoT network: From AWGN channel to THz band," *IEEE Internet Things J.*, vol. 7, no. 4, pp. 3378–3388, Apr. 2020.

[2] S. Han, C. Lin, Z. Xu, and C. Rowell, "Large-scale antenna systems with hybrid analog and digital beamforming for millimeter wave 5G," *IEEE Commun. Mag.*, vol. 53, no. 1, pp. 186–194, Jan. 2015.

[3] C. Qi, P. Dong, W. Ma, H. Zhang, Z. Zhang, and G. Y. Li, "Acquisition of channel state information for mmWave massive MIMO: Traditional and machine learning-based approaches," *Sci. China Inf. Sci.*, vol. 64, no. 8, Aug. 2021, Art. no. 181301.

[4] B. A. Bash, D. Goeckel, and D. Towsley, "Limits of reliable communication with low probability of detection on AWGN channels," *IEEE J. Sel. Areas Commun.*, vol. 31, no. 9, pp. 1921–1930, Sep. 2013.

[5] M. V. Jamali and H. Mahdavifar, "Covert millimeter-wave communication: Design strategies and performance analysis," *IEEE Trans. Wireless Commun.*, vol. 21, no. 6, pp. 3691–3704, Jun. 2022.

[6] C. Wang, Z. Li, and D. W. K. Ng, "Covert rate optimization of millimeter wave full-duplex communications," *IEEE Trans. Wireless Commun.*, vol. 21, no. 5, pp. 2844–2861, May 2022.

[7] W. Ci, C. Qi, G. Y. Li, and S. Mao, "Hybrid beamforming design for covert multicast mmWave massive MIMO communications," in *Proc. IEEE Global Commun. Conf. (GLOBECOM)*, Madrid, Spain, Dec. 2021, pp. 1–6.

[8] J. Zhang, X. Chen, M. Li, and M. Zhao, "Optimized throughput in covert millimeter-wave UAV communications with beam sweeping," *IEEE Wireless Commun. Lett.*, vol. 10, no. 4, pp. 720–724, Apr. 2021.

[9] J. Zhang et al., "Joint beam training and data transmission design for covert millimeter-wave communication," *IEEE Trans. Inf. Forensics Security*, vol. 16, pp. 2232–2245, 2021.

[10] C. Qi, K. Chen, O. A. Dobre, and G. Y. Li, "Hierarchical codebook-based multiuser beam training for millimeter wave massive MIMO," *IEEE Trans. Wireless Commun.*, vol. 19, no. 12, pp. 8142–8152, Dec. 2020.

[11] S. Yan, B. He, Y. Cong, and X. Zhou, "Covert communication with finite blocklength in AWGN channels," in *Proc. IEEE Int. Conf. Commun. (ICC)*, Paris, France, May 2017, pp. 1–6.

[12] K. T. Phan, S. A. Vorobyov, N. D. Sidiropoulos, and C. Tellambura, "Spectrum sharing in wireless networks via QoS-aware secondary multicast beamforming," *IEEE Trans. Signal Process.*, vol. 57, no. 6, pp. 2323–2335, Jun. 2009.

Authorized licensed use limited to: Southeast University. Downloaded on May 10,2023 at 08:07:31 UTC from IEEE Xplore. Restrictions apply.